IEEE Access
Multidisciplinary | Rapid Review | Open Access Journal

Received May 2, 2019, accepted July 19, 2019, date of publication July 26, 2019, date of current version August 12, 2019.

Digital Object Identifier 10.1109/ACCESS.2019.2931286

Study on the Charge Transfer Criterion for the Pole-to-Ground Fault in DC Distribution Networks

BOTONG LI, XIANG REN, AND BIN LI

Key Laboratory of Smart Grids , School of Electrical and Information Engineering, Ministry of Education, Tianjin University, Tianjin 300072, China

Corresponding author: Bin Li (libin_tju@126.com)

This work was supported in part by the National Natural Science Foundation of China under Grant 51677125 and in part by the National Natural Science Foundation of China Smart Grid Joint Foundation under Grant U1866205.

ABSTRACT After a pole-to-ground fault occurs in the DC distribution network using low current grounding, the fault pole voltage drops while that of the non-fault pole rises, which is harmful to equipment insulation and operational safety. Therefore, it is necessary to accurately identify and locate faults with protection equipment. In order to solve the pole-to-ground fault in DC distribution networks using low current grounding, the characteristics of different fault current loops are studied. The distributed capacitance discharging loop at the fault pole, the distributed capacitance charging loop at the non-fault pole, and the feeding of system grounding loop current into the fault grounding point current are analyzed. On this basis, a protection criterion for distinguishing the internal fault from the external fault by the amount of transferred charges, which can be calculated based on the transient differential current, is proposed in this paper. The simulation results show that the proposed pole-to-ground fault criterion can reliably identify the fault line while being immune to the influence of transitional resistance.

INDEX TERMS DC power distribution, pole-to-ground fault, capacitance charge, fault line location.

I. INTRODUCTION

DC distribution is a new type of power distribution technology based on the voltage source type modular multilevel converter (MMC) [1]–[3]. Compared with AC distribution, DC power distribution has many advantages in terms of power supply capacity, quality and reliability [4]–[6]. Up to now, many countries including China have carried out different forms of research on DC distribution theories and relevant demonstration projects. The DC power distribution system is gradually becoming a worldwide hotspot in smart gird research and construction [7], [8].

The voltage of the DC distribution network generally ranges from several kilovolts to several tens of kilovolts, mostly in the form of unipolar symmetrical wiring. To ensure the reliability of the system, the low current grounding method is generally adopted at the neutral point of the system [9], [10]. When a pole-to-ground fault occurs, the fault current is small, and the voltage at the fault pole will decrease to close to zero while that at the non-fault pole will increase to about twice of the rated voltage. The rise of voltage at the non-fault pole will cause a large overvoltage in the system, posing a great threat to the safe operation of relevant lines and electrical equipment [11], [12]. Therefore, it is necessary for the line protection devices of a DC distribution network to accurately identify and locate the pole-to-ground fault and isolate the fault line in time to ensure the operational safety of the system [13], [14].

Some research revolving around the protection principles and methods of the pole-to-ground fault in a DC distribution network has been carried out and preliminary results have been achieved. Considering the fault current is too small, a method to identify the pole-to-ground fault by detecting the steady-state leakage current, which will not be affected by the capacitance-to-ground is proposed in [15], but it requires high precision for the detecting equipment. A method of detecting and identifying the pole-to-ground fault by injecting an alternating current into the line when a fault occurs is proposed in [16]. However, this method is subject to the interference of noise, and additional signal generation and detection equipment will be needed. In [17], after detecting a fault, the converter sub-modules will send a traveling

The associate editor coordinating the review of this manuscript and approving it for publication was Yanzheng Zhu.

wave pulse to the line, according to which the line protection equipment can then recognize and locate the fault, but this method requires an additional sub-module pulse control unit, the high accuracy on the pulse signal arrival time, as well as high sampling frequency for the related protection devices.

Given the difficulty in detecting weak fault currents and limitations of the signal injection method, some scholars have also carried out research on fault characteristics and analyzing methods, and have made some achievements. In [18], a pole-to-ground fault identification method by calculating the correlation between currents at the positive and negative poles using the Pearson correlation coefficient is proposed, but its sensitivity can be affected by transitional resistance. In [19], the short-time energy of the differential current is used to expand difference between the transient characteristics of electrical quantity during an internal fault and those during an external fault, which can achieve the purpose of distinguishing fault lines. However, comparison of the differential currents in every line segment is needed, with additional communication and logic modules for relay protection and the high synchronization of electrical data required. In [20], the zero-sequence fault network is analyzed under the condition of a medium-voltage DC distribution system with high-impedance grounding or ungrounded neutral points. Based on this, it proposes a fault feeder line location method by calculating the line capacitance-to-ground. The voltage and current of lines within specific frequency bands are needed to calculate the capacitance, increasing the calculation complexity. Literature above indicates that research on the identification and location for the pole-to-ground fault in DC distribution networks is still facing difficulties including high complexity and demanding equipment requirements.

In this paper, the charging and discharging currents of the cable capacitance-to-ground are analyzed, and the difference between the amount of transferred capacitance charges during an internal fault and that during an external fault is studied. On this basis, a protection method for the pole-to-ground fault based on the amount of transferred capacitance charges is proposed. The accuracy and practicability of the method are verified by a DC distribution network model built in PSCAD/EMTDC.

II. TYPICAL STRUCTURE AND CABLE PARAMETER CHARACTERISTICS OF DC DISTRIBUTION NETWORKS

A. TYPICAL TOPOLOGY OF DC DISTRIBUTION NETWORKS

Typical DC distribution networks can be divided into the radial type, the ring type and the double-ended type. With a comprehensive consideration of the system reliability, the complexity of operation control and protection configuration, this paper takes the double-ended DC distribution network as an example for analysis. The line between the power supplies at both ends are divided into three sections. The typical system structure is shown in Fig.1 and the basic structure of a MMC converter station is shown in Fig.2 [21].

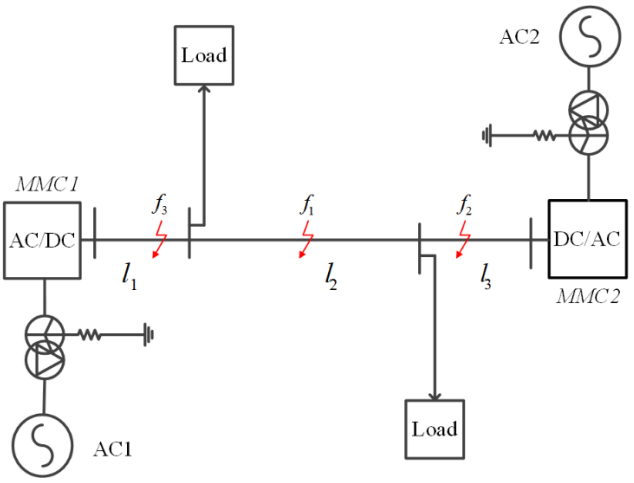

FIGURE 1. Double-ended DC power distribution system.

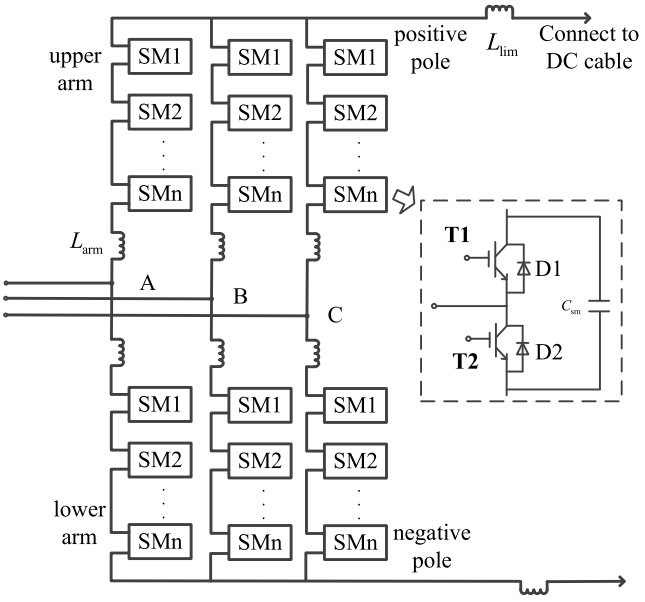

FIGURE 2. Basic structure of a MMC converter station.

The results of analysis also apply to other types of DC distribution networks.

In Fig.1, the DC power distribution system adopts the unipolar symmetrical wiring. The converter adopts the MMC topology of a half bridge submodule; Converter station *MMC1* adopts constant active power control and constant reactive power control, while converter station *MMC2* adopts constant DC voltage control and constant reactive power control; The current limiting reactor next to the exit of the DC bus is optional based on the actual situation; Taking the operating condition and reliability requirement of DC distribution networks in cities or industrial parks into full account, DC cables are used as transmission lines.

The parameters of the DC power distribution system of the actual project are shown in Table 1 [22].

TABLE 1. Parameters of double-ended DC distribution system.

system parameter	parameter value
rated DC voltage / kV	±10
rated AC voltage /kV	10
transformation ratio	11:1
amount of coverter levels	24
submodule capacitance / μ F	30
bridge arm inductance / mH	2.5
current limiting inductance / mH	8
total length of cable line /km	20
rated capacity /MVA	25
system grounding resistance / Ω	2500

B. NEUTRAL POINT GROUNDING AND CABLE PARAMETERS

In the DC power distribution system using MMC converters, in order to maintain the symmetry of the positive and negative voltages of the DC bus, the grounding point is generally the reference point for zero potential in the system. At present, typical grounding methods used in actual projects mainly include [23]:

(1) DC side grounding: two identical clamping resistors are connected in series between the positive and negative buses, and the system is grounded through the connection point of the two clamping resistors;

(2) AC side grounding: ground through large resistance at the neutral point of the star-shaped transformer winding or through resistance at the parallel star-shaped reactance on the secondary side of the connecting transformers.

The above grounding methods all belong to the low current grounding and the fault current of pole-to-ground fault is small. In this paper, the characteristics of the pole-to-ground fault are analyzed under the condition where the neutral point is grounded through the transformer resistance, as shown in Fig.1. The analysis results are applicable to other grounding methods.

The cable capacitance is much greater than that of the overhead line. Based on the geometric parameters and physical characteristics of the cable and the overhead line in actual projects, a DC line model is built in PSCAD/EMTDC. The simulation is conducted using the frequency dependent model at 0.001 Hz. The capacitance parameters of the DC cable and the overhead line are calculated, as shown in Table 2.

TABLE 2. Capacitance parameters of 10 kV DC cable line and overhead line.

	cable line	overhead line
Capacitance-to-ground μ F/km	0.618	0.00782
Capacitance between poles μ F/km	0	0.0122

Comparing the capacitance parameters of the cable line and the overhead line, it can be found that the capacitance-to-ground per unit length of the cable is several tens times higher than that of the overhead line. Therefore, the charging and discharging currents in the cable line in the transient stage after a pole-to-ground fault should be much larger than those in the overhead line.

III. CURRENT CHARACTERISTICS ANALYSIS OF THE POLE-TO-GROUND FAULT

When a pole-to-ground fault occurs on the line, the reference point for zero potential in the DC distribution network is transferred from the neutral point of transformers to the fault grounding point. The fault pole voltage drops, and the non-fault pole voltage rises, while the voltage between the poles remains basically unchanged [18]. With no direct grounding point in the DC system, the pole-to-ground fault current would not be large [19]. However, the change in voltages of the positive and negative lines will cause charging and discharging of the ground cable capacitance. Transient process of the pole-to-ground fault is analyzed below.

In this paper, the direction of the inflow current to the node or the generalized node is determined as the positive direction, as Fig.3 shows. The bus or fault point can be regarded as a node, and the line can be regarded as a generalized node.

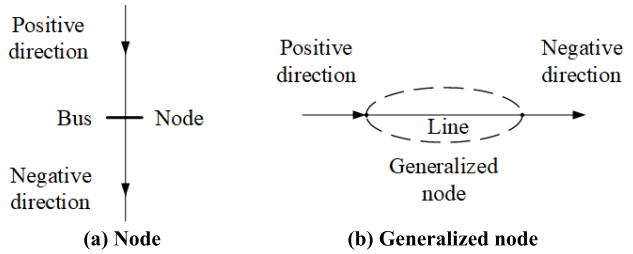

FIGURE 3. Positive direction of current.

Taking the positive pole-to-ground fault as an example, the fault current equivalent circuit of a grounding fault is shown in Fig.4. The three line segments are considered as a unified line because the specific line segment on which the fault occurs does not affect the analysis results in this section.

The fault current at the fault grounding point is mainly composed of the transformer neutral point grounding current, the capacitance-to-ground discharging current at the fault pole and the capacitance-to-ground charging current at the non-fault pole. The current loops are shown by dotted lines ①, ②, ③ in Fig.4. i_{1_MMC1}, i_{1_MMC2}, i_{2_MMC1}, i_{2_MMC2}, i_{3_MMC1}, and i_{3_MMC2} are fault currents in loops ①, ②, ③ respectively on the *MMC1* and *MMC2* sides; C_c and L_c are respectively the equivalent capacitance and equivalent reactance of the converter bridge arm, which can be calculated by the formula given in [24]. L_t is the transformer reactance; C_{cb-P} and C_{cb-N} are the equivalent capacitances of the positive and negative cable lines per unit length; R_{cb} and L_{cb} are the resistance and inductance of the positive and negative cable lines per unit length; x is the total length of the three segments of cable lines; x_{f-1} and x_{f-2} are the line lengths from the point of the fault to the exits of *MMC1* and *MMC2*, respectively.

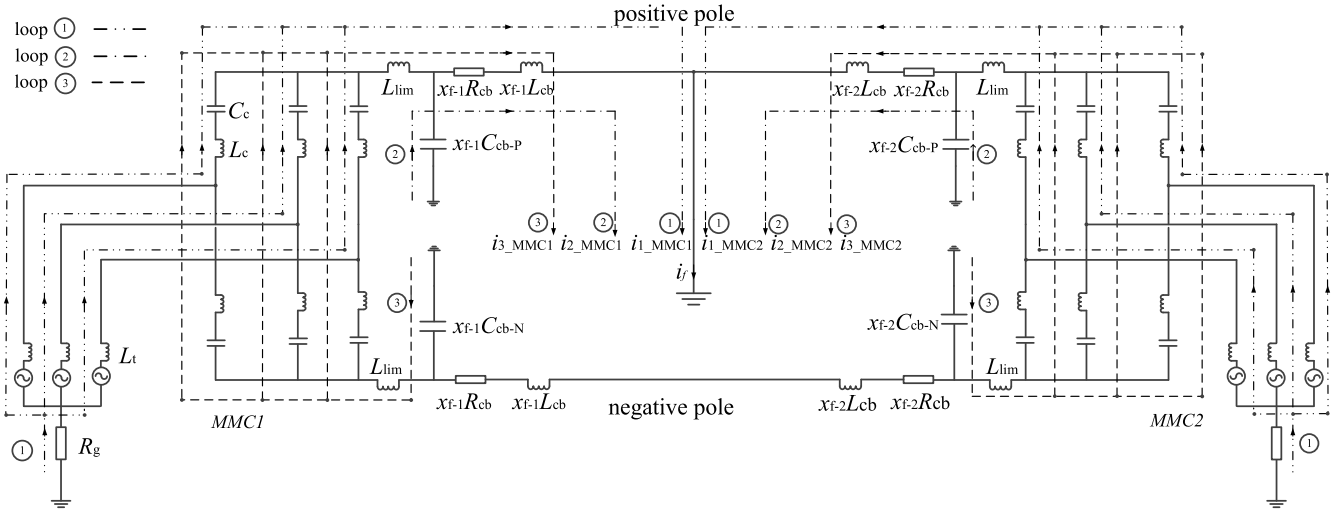

FIGURE 4. Equivalent loop diagram of a pole-to-ground fault.

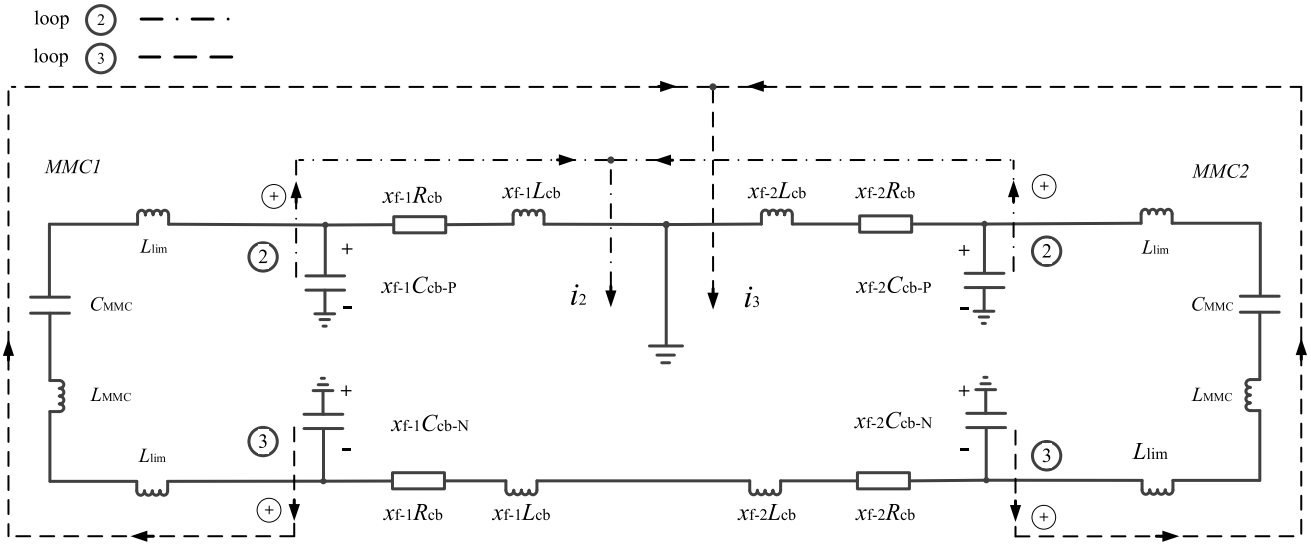

FIGURE 5. Simplified circuit for positive pole-to-ground fault.

The follows are the analysis of each loop current:

(1) The corresponding transformer neutral point grounding current to loop ①: In normal operation, $U_{dc}/2$ and $-U_{dc}/2$, the positive and negative voltages on the DC side respectively are symmetrical. According to the converter modulation principle, U_N of the transformer neutral point on the AC side, as the reference point for zero potential in the system, remains at zero. After the positive grounding fault occurs, the reference point will be transferred from the transformer neutral point to the fault grounding point [19].

Since neutral point grounding resistance R_g is much larger than line impedance xR_{cb}, the transformer neutral point voltage will decrease close to negative pole voltage $-U_{dc}/2$. The steady-state fault current flowing through the neutral points of the connecting transformers on both sides of *MMC1* and *MMC2* is shown as (1):

$$\begin{aligned} i_1 &= i_{1\_MMC1} + i_{1\_MMC2} \\ &= \frac{U_{dc}/2}{R_g + x_{f\text{-}1}R_{cb}} + \frac{U_{dc}/2}{R_g + x_{f\text{-}2}R_{cb}} \\ &\approx \frac{U_{dc}}{R_g} \end{aligned} \tag{1}$$

According to the grounding resistance parameters provided in Table 1 in Section II, the steady-state fault current provided by the neutral point of transformer i_1 is about 8A, which can be ignored since it's very small.

Therefore, loop ① can be ignored and the simplified fault circuit is shown in Fig.5.

In Fig.5, C_{MMC} is the integrated equivalent capacitance of the upper and lower arms of the MMC stations, whereas L_{MMC} the integrated equivalent reactance [25].

(2) The corresponding capacitance-to-ground discharging current at the fault pole to loop ② in Fig.4 and Fig.5: When the positive pole is grounded, its voltage will drop and the line capacitance will discharge. The discharging current flows from the line capacitance at the fault pole to the fault ground point. According to the capacitance discharging current formula, capacitance current i_2 is:

$$\begin{aligned} i_2 &= i_{2\_\mathrm{MMC1}} + i_{2\_\mathrm{MMC2}} \\ &= (-x_{\mathrm{f\text{-}1}} C_{\mathrm{cb\text{-}P}} \frac{du_{\mathrm{posi}}}{dt}) + (-x_{\mathrm{f\text{-}2}} C_{\mathrm{cb\text{-}P}} \frac{du_{\mathrm{posi}}}{dt}) \\ &= -xC_{\mathrm{cb\text{-}P}} \frac{du_{\mathrm{posi}}}{dt} \end{aligned} \tag{2}$$

u_{posi} is the transient voltage of the positive pole, which will become a steady value close to zero after the transient process. The capacitance discharging current in the positive line can be regarded as positive charges flowing from the positive electrode of the capacitance to the fault ground point. When the positive voltage reaches the steady state, the amount of transferred charges can then be calculated by:

$$\begin{aligned} Q_2 &= \int_{t_0}^{t_0+\Delta t} i_2 dt = \int_{t_0}^{t_0+\Delta t} -xC_{cb-\mathrm{P}} du_{posi} \\ &= xC_{cb-\mathrm{P}} \cdot (-u_{posi}) \Big|_{U_{dc}/2}^{0} \\ &= xC_{cb-P} U_{dc}/2 \end{aligned} \tag{3}$$

Q_2 is positive, indicating positive charges flow from the line into the fault point.

(3) The corresponding capacitance-to-ground charging current at the non-fault pole to loop ③ in Fig.4 and Fig.5: When the positive pole is grounded, the voltage of the negative pole will rise and eventually reach $-U_{\mathrm{dc}}$, which will charge its capacitance-to-ground during this process. The charging current flows from the negative line through the MMC stations to the fault ground point at the positive pole. According to the capacitance discharging current formula, capacitance current i_3 is:

$$\begin{aligned} i_3 &= i_{3\_\mathrm{MMC1}} + i_{3\_\mathrm{MMC2}} \\ &= (-x_{\mathrm{f\text{-}1}} C_{\mathrm{cb\text{-}N}} \frac{du_{\mathrm{nega}}}{dt}) + (-x_{\mathrm{f\text{-}2}} C_{\mathrm{cb\text{-}N}} \frac{du_{\mathrm{nega}}}{dt}) \\ &= -xC_{\mathrm{cb\text{-}N}} \frac{du_{\mathrm{nega}}}{dt} \end{aligned} \tag{4}$$

u_{nega} is the transient voltage of the negative pole, which will become a steady state value close to $-U_{\mathrm{dc}}$ after the transient process. The capacitance charging current in the positive line can be regarded as positive charges flowing from the negative electrode of the capacitance to the fault ground point. When the negative voltage reaches the steady state, the amount of transferred charges can then be calculated by:

$$\begin{aligned} Q_3 &= \int_{t_0}^{t_0+\Delta t} i_3 dt = xC_{cb-N} \int_{t_0}^{t_0+\Delta t} -du_{nega} \\ &= xC_{cb-N} \cdot (-u_{nega}) \Big|_{-U_{dc}/2}^{-U_{dc}} \\ &= xC_{cb-N} U_{dc}/2 \end{aligned} \tag{5}$$

Q_3 being positive indicates that positive charges flow from the line into the fault point.

Based on the fault currents on the *MMC1* side and the *MMC2* side, after the fault occurs, fault current i_f flowing through the fault grounding point is:

$$i_{\mathrm{f}} = i_1 + i_2 + i_3 \tag{6}$$

i_{f} is in oscillating attenuation. Its transient process is related to the position of the fault point, the line impedance parameters, the current limiter inductance, the converter equivalent capacitance and the inductance, which causes difficulty for a precise expression. However, by leaving fault current i_1 flowing from the neutral points of the connecting transformers aside and integrating the other parts, the amount of charges flowing into the ground fault point can be obtained:

$$Q = \int_{t_0}^{t_0+\Delta t} i_{\mathrm{f}} dt \approx \int_{t_0}^{t_0+\Delta t} (i_2 + i_3) dt = Q_2 + Q_3 \tag{7}$$

As can be seen from (3), (5) and (7), after the grounding fault reaches the steady state after the transient process, the amount of charges flowing into the fault point is certain, which is only related to the capacitance of the positive and negative cable lines and the line operating voltage.

IV. ANALYSIS OF CHARGE TRANSFER CHARACTERISTICS OF THE INTERNAL AND EXTERNAL FAULTS

Taking the protection of line l_2 as an example, the line can be regarded as a generalized node. The relevant protections are at its M end and N end. In Fig.1, f_1 is the pole-to-ground fault occurring at the positive pole of line l_2, while f_2 and f_3 of line l_3 and line l_1. i_m and i_n are the currents flowing through the protection at two ends of line l_2.

A. INTERNAL POLE-TO-GROUND FAULT

When the fault f_1 occurs at the positive pole of line l_2l$_2$, the capacitance current flowing path is shown in Fig.6.

According to the analysis in Section III, currents i_{m} and i_{n} on both sides of the fault pole after the positive fault in line l_2 are composed of its load current and the line capacitance charging and discharging currents in loop ② and loop ③:

$$\begin{cases} i_{\mathrm{m}} = i_{\mathrm{load}} + i_{2\_l1} + i_{3\_\mathrm{MMC1}} \\ i_{\mathrm{n}} = -i_{\mathrm{load}} + i_{2\_l3} + i_{3\_\mathrm{MMC2}} \end{cases} \tag{8}$$

In the (8), the negative sign indicates that the current direction is opposite to the current positive direction; i_{load} is the load current of line l_2; i_{2_l1} is the capacitance discharging current at the positive pole of line l_1; i_{3_MMC1} is the capacitance charging current in all negative lines flowing through

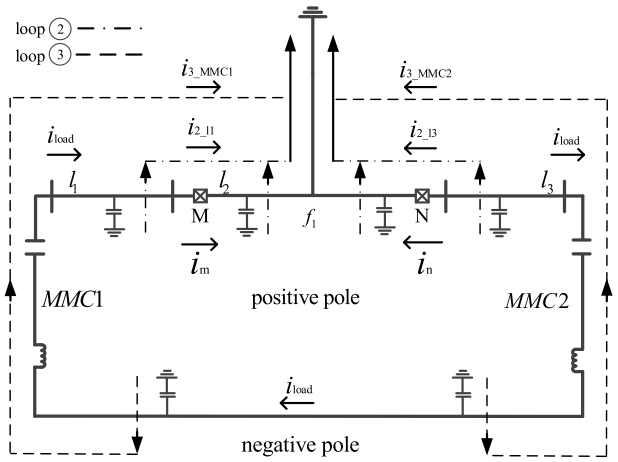

FIGURE 6. Internal positive pole-to-ground fault in l_2.

converter station *MMC1* to the fault grounding point; i_{2_l3} is the capacitance discharging current at the positive pole of line l_3; i_{3_MMC2} is the capacitance charging current in all negative lines flowing through converter station *MMC2* to the fault grounding point.

Calculate the differential current of line l_2:

$$\begin{aligned} i_{diff} &= i_m + i_n \\ &= i_{3\_MMC1} + i_{2\_l1} + i_{3\_MMC2} + i_{2\_l3} \\ &= i_{3\_l1} + i_{3\_l2} + i_{3\_l3} + i_{2\_l1} + i_{2\_l3} \end{aligned} \tag{9}$$

In formula (9), i_{diff} can be regarded as the current flowing into the generalized node of line l_2; i_{3_l1}, i_{3_l2} and i_{3_l3} are respectively the capacitance charging currents of the negative sections of lines l_1, l_2 and l_3; i_{2_l1} and i_{2_l3} are respectively the capacitance discharging currents of the positive sections of lines l_1 and line l_3.

Integrate differential current i_{diff} when the charging and discharging reach the steady state:

$$\begin{aligned} \int_t^{t+\Delta t} i_{diff}dt &= \int_t^{t+\Delta t} i_m + i_n dt \\ &= \int_t^{t+\Delta t} (i_{3\_l1} + i_{3\_l2} + i_{3\_l3} + i_{2\_l1} + i_{2\_l3})dt \\ &= \int_t^{t+\Delta t} (i_{3\_l1} + i_{3\_l2} + i_{3\_l3})dt \\ &\quad + \int_t^{t+\Delta t} (i_{2\_l1} + i_{2\_l3})dt \\ &= Q_{nega\_(l1+l2+l3)} + Q_{posi\_(l1+l3)} \end{aligned} \tag{10}$$

In (10), Δt is the time from the fault occurs to the line capacitance current decaying to zero; $Q_{nega\_(l1+l2+l3)}$ is the amount of capacitance charging charges in all negative lines; $Q_{posi\_(l1+l3)}$ is the capacitance discharging charges in the positive sections of lines l_1 and line l_3.

The DC distribution network model in Fig.1 is used in PSCAD/EMTDC for simulation. At time t_0, an internal positive pole-to-ground fault occurs on line l_2 since which the integration differential current i_{diff} starts. The calculation result is shown in Fig.7.

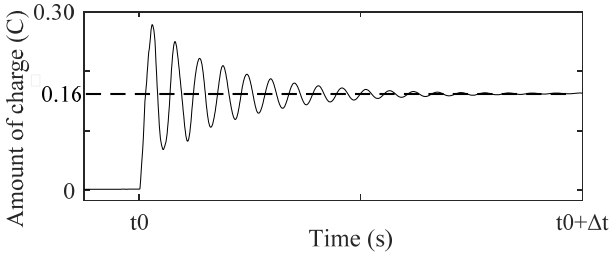

FIGURE 7. Integration result of i_{diff} after internal fault in the l_2.

As can be seen from Fig.7, the calculated amount of charges gradually becomes stable as the integration proceeds, which indicates the completion of capacitance charging and discharging as well as the charge transfer process.

According to (3), (5) and (7), the amount of transferred charges Q is related to the line voltage fluctuation and all the distributed capacitances except the fault pole of the line:

$$\begin{aligned} Q &= Q_{nega\_(l1+l2+l3)} + Q_{posi\_(l1+l3)} \\ &= (l_1 + l_2 + l_3)C_{cb}U_{dc}/2 + (l_1 + l_3)C_{cb}U_{dc}/2 \end{aligned} \tag{11}$$

Q being positive suggests that the charges flow into generalized node l_2. Substitute the values of line length, unit capacitance and voltage parameters into (11), $Q \approx 0.16\ C$. As shown by the dotted line in Fig.7, the theoretical calculation result of the charges is the same as the final integration result of the differential current.

B. EXTERNAL POLE-TO-GROUND FAULT

When fault f_2 occurs on the positive sections of external area in line l_3, the capacitance current flowing through protection installation points M and N is as shown in Fig.8.

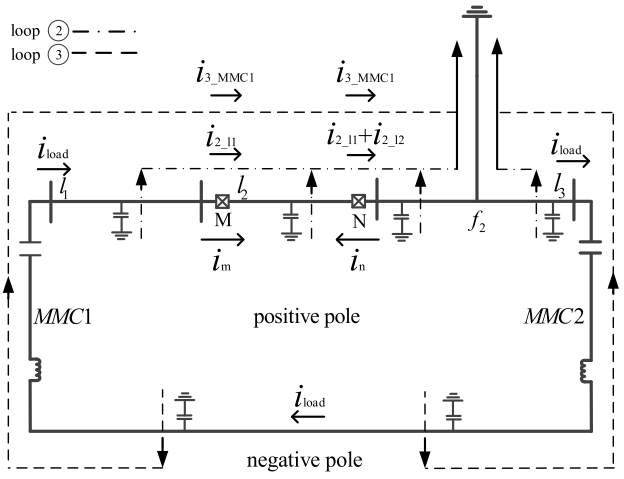

FIGURE 8. External positive pole-to-ground fault in line l_3.

As can be seen in Fig.8, the measured currents i_m and i_n flowing through the protection at both ends of

line l_2 are:

$$\begin{cases} i_{\mathrm{m}} = i_{\mathrm{load}} + i_{2\_l1} + i_{3\_\mathrm{MMC1}} \\ i_{\mathrm{n}} = -i_{\mathrm{load}} - (i_{2\_l1} + i_{2\_l2}) - i_{3\_\mathrm{MMC1}} \end{cases} \tag{12}$$

In (12), i_{2_l1} is the capacitance discharging current in the positive section of line l_1; i_{2_l2} is the capacitance discharging current in the positive section of line l_2; i_{3_MMC1} is the capacitance charging current flowing through converter station *MMC1* to the fault ground point in all negative lines.

Differential current i_{diff} flowing through line l_2 is:

$$\begin{aligned} i_{\mathrm{diff}} &= i_{\mathrm{m}} + i_{\mathrm{n}} \\ &= i_{2\_l1} - (i_{2\_l1} + i_{2\_l2}) \\ &= -i_{2\_l2} \end{aligned} \tag{13}$$

Integrate differential current i_{diff}:

$$\int_t^{t+\Delta t} i_{\mathrm{diff}} dt = \int_t^{t+\Delta t} -i_{2\_l2} dt = -Q_{\mathrm{posi\_l2}} \tag{14}$$

In (14), Δt is the time from the fault occurs to the line capacitance current decaying to zero; $Q_{\mathrm{posi\_l2}}$ is the amount of capacitance discharging charges of l_2 positive sections, which is a negative value. At time t, the positive grounding fault occurs on line l_3, integrate i_{diff} and the calculation result is shown in Fig.9.

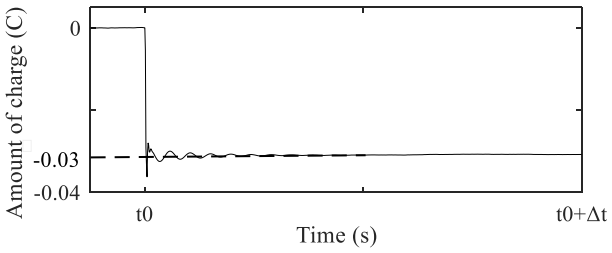

FIGURE 9. Integration result of $\mathbf{i_{diff}}$ after external fault in the $\boldsymbol{l_3}$.

It can be seen from Fig.9 that as the integration proceeds, the calculated amount of charges gradually becomes stable, which indicates the completion of capacitance charging and discharging as well as the charge transfer process. According to (3), the calculated amount of charges is related to the line voltage and the positive pole distributed capacitance of the protected line l_2, which is:

$$Q = -Q_{\mathrm{posi\_l2}} = -l_2 C_{\mathrm{cb}} U_{\mathrm{dc}} / 2 \tag{15}$$

Q being negative suggests that the charges flow out of generalized node l_2. Substitute the values of line length, unit capacitance and voltage parameters into (15), $Q \approx -0.03$. Fig.9 shows that the theoretical calculation result of the charges is the same as the final integration result of the differential current.

When the external pole-to-ground fault f_3 occurs on line l_1, the integration result of the differential current is the same as the fault analysis result of line l_3:

$$\begin{aligned} \int_t^{t+\Delta t} i_{\mathrm{diff}} dt &= \int_t^{t+\Delta t} (i_{\mathrm{m}} + i_{\mathrm{n}}) dt \\ &= \int_t^{t+\Delta t} \big[(i_{\mathrm{load}} - i_{3\_\mathrm{MMC2}} - i_{2\_l2} - i_{2\_l3}) \\ &\quad + (-i_{\mathrm{load}} + i_{3\_\mathrm{MMC2}} + i_{2\_l3}) \big] dt \\ &= \int_t^{t+\Delta t} -i_{2\_l2} dt \\ &= -Q_{\mathrm{posi\_l2}} \end{aligned} \tag{16}$$

The result is still the negative of the capacitance discharging charges of l_2 positive sections. At time t, the positive grounding fault occurs in line l_1. Integrate i_{diff} with time t, and the calculation result is shown in Fig.10.

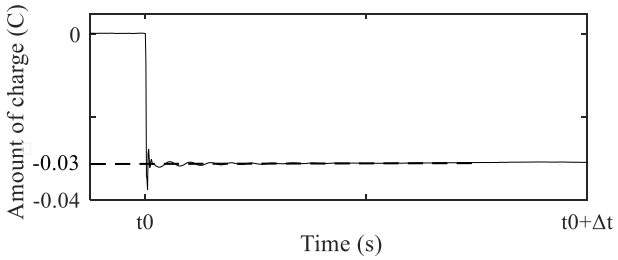

FIGURE 10. Integration result of $\mathbf{i_{diff}}$ after external fault in line $\boldsymbol{l_1}$.

Fig.10 shows that as the integration proceeds, the calculated amount of charges gradually becomes stable, which indicates the completion of capacitance charging and discharging as well as the charge transfer process. According to (3), the calculated amount of charges is related to the line voltage and the positive pole distributed capacitance of the protected line l_2, which is:

$$Q = -Q_{\mathrm{posi\_l2}} = -l_2 C_{\mathrm{cb}} U_{\mathrm{dc}} / 2 \tag{17}$$

Q being negative suggests that the charges flow out of generalized node l_2. Take The line length, unit capacitance and voltage parameters into the formula, $Q \approx 0.03$. Fig.10 shows that the theoretical calculation result of the charges is the same as the final integration result of the differential current.

Based on the above analysis, it can be seen that when the pole-to-ground fault is internal, the amount of transferred charges calculated by integrating the differential current is the sum of the capacitance charging charges at the non-fault poles of all lines and the capacitance discharging charges at the fault pole of the external line; When the pole-to-ground fault is external, the amount of transferred charges is the negative value of the distributed capacitance discharging charges at the fault pole of the internal line. The two amounts differ widely, and therefore can distinguish the internal fault from the external fault in DC lines. This conclusion is also applicable to DC distribution networks of other topology types.

V. PROTECTION METHOD FOR THE POLE-TO-GROUND FAULT

A. INITIATION CRITERION OF PROTECTION

Since the voltage at the fault pole will decrease to close to zero in a short time after a fault, the line voltage change can function as the protection start element:

$$|u| > K_{\text{rel}} \cdot U_{\text{n}} \tag{18}$$

Δu is the voltage variation at the positive or negative pole, which can be obtained by calculating the difference between two sample voltages during a certain time interval. In this paper, Δu is calculated by subtracting the voltage value 3 ms before from the current voltage value. U_n is the rated line voltage; K_{rel} is the reliability coefficient and its value ranges from 0.2 to 0.5. When the above criterion has been met 3-6 times, the protection starts, and the time is the fault occurrence time.

B. FAULT-POLE IDENTIFICATION CRITERION

According to the voltage fluctuation during a pole-to-ground fault, the fault pole can be identified by the criterion in reference [26]:

$$k = |\frac{u_{\text{P}}}{u_{\text{N}}}| \tag{19}$$

$$\begin{cases} \text{positive pole grounding fault} : k < 1/k_{\text{set}} \\ \text{negative pole grounding fault} : k > k_{\text{set}} \end{cases} \tag{20}$$

u_P and u_{N} are the DC voltages of the positive and negative poles respectively; k is the ratio between the positive voltage and the negative voltage; k_{set} is the setting value for the fault pole selection criterion. Set k_{set} more than 2 to meet the reliability requirements. This article only discusses the case of the pole-to-ground fault, so the identifying method of pole-to-pole fault will not be included.

C. IDENTIFICATION CRITERION FOR INTERNAL FAULTS AND EXTERNAL FAULTS

According to the analysis on the differential current and the amount of transferred charges in Section III and Section IV, it can be concluded that the amount of transferred charges can be used to distinguish different grounding faults. In this paper, the amount of transferred charges is obtained by integrating the differential currents at the positive and negative poles to identify the fault, as shown in (21). The identification criterion for the internal fault is based on the amount of charges, as shown in (22):

$$Q_t = \int_{t_0}^{t_0+\Delta t} i_{\text{diff}} dt \tag{21}$$

$$Q_{\text{t}} \geq Q_{\text{set}}\text{: Internal fault} \tag{22}$$

In this formula, i_{diff} is the differential current of line l_2; Q_t is the integrated value of the differential current, which is the amount of transferred charges; t_0 is the starting time of protection; Δt is the integration time after the protection starts; Q_{set} is the threshold of the fault identification criterion which is set to half the total of transferred charges after both an internal fault and an external fault, which is:

$$\begin{aligned} Q_{\text{set}} &= \left[(Q_{\text{nega\_(l1+l2+l3)}} + Q_{\text{posi\_(l1+l3)}}) - Q_{\text{posi\_l2}}\right]/2 \\ &= \left[(l_1 + l_2 + l_3)C_{\text{cb}}U_{\text{dc}}/2 + (l_1 + l_3)C_{\text{cb}}U_{\text{dc}}/2 - l_2 C_{\text{cb}}U_{\text{dc}}/2\right]/2 \\ &= (l_1 + l_3)C_{\text{cb}}U_{\text{dc}}/2 \end{aligned} \tag{23}$$

In (23), C_{cb} is the line capacitance per unit length; $U_{\text{dc}}/2$ is the DC line voltage variation. As can be seen, the setting value Q_{set} is the amount of capacitance charging charges in non-fault lines.

VI. SIMULATION AND VERIFICATION

A. SIMULATION RESULTS

The DC power distribution system shown in Fig.1 is built in PSCAD/EMTDC. The length of lines l_1, l_2 and l_3 is 5 km. DC cables are used as the transmission line, simulated by frequency dependent model.

Set the fault to occur at 1.3 s; The data sampling frequency is 5 kHz; Reliability coefficient K_{rel} of the initiation criterion is 0.2; The setting value of the fault-pole identification criterion k_{set} is 2; Setting value Q_{set} is obtained by substituting the line parameters into (23), and the value is 0.09 C; In order to get a fixed result, integration time Δt is set to 20 ms. Set the l_2 internal positive pole grounding fault at f_1, and the calculation results are as shown in Fig.11. The dotted lines are the thresholds of the initiation criterion, the fault pole identification criterion and the fault identification criterion.

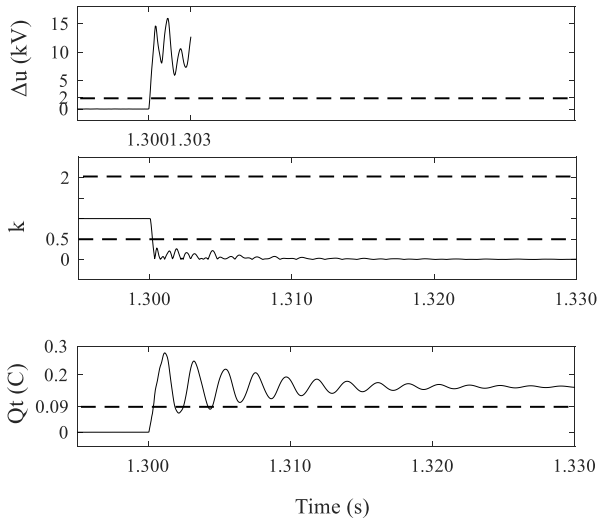

FIGURE 11. Internal positive pole-to-ground fault in line l_2.

As can be seen from Fig.11, when there is an internal positive pole grounding fault, initiation criterion $\Delta u > 2kV$, and the protection starts; fault-pole identification criterion $k < 0.5$, suggesting that there is a pole-to-ground fault at the positive pole; At time 1.320 s, fault identification criterion $Q_{\text{t}} > 0.09$C, indicating that the fault is an internal one.

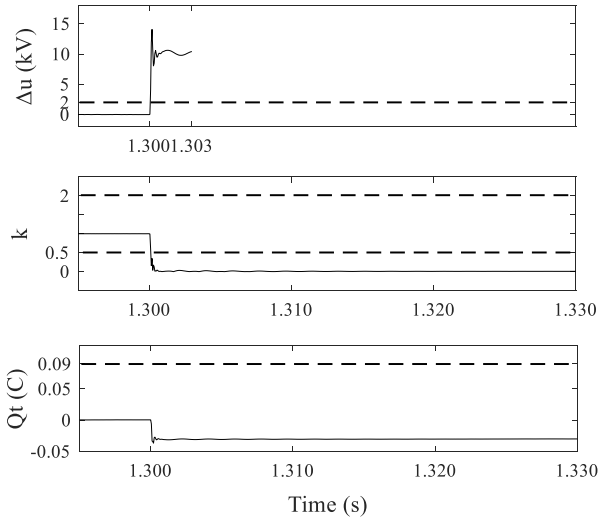

FIGURE 12. External positive pole-to-ground fault in line l_3.

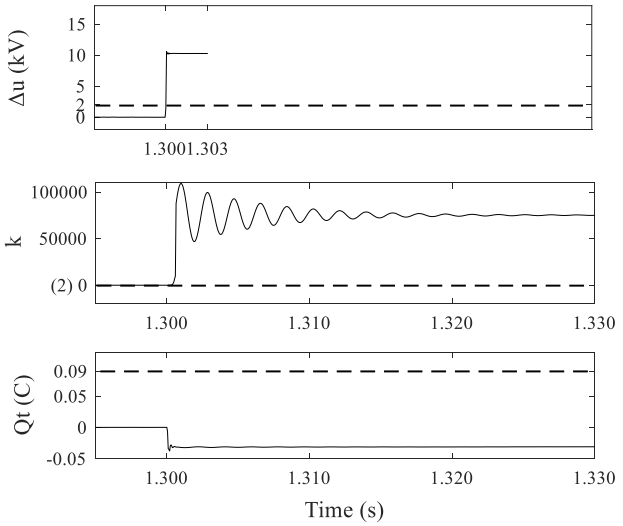

FIGURE 13. External negative pole-to-ground fault in line l_1.

Set the external positive grounding fault in line l_3 at f_2, and the results are as shown in Fig.12.

As can be seen from Fig.12, when there is an external positive grounding fault, initiation criterion $\Delta u > 2kV$, and the protection starts; fault-pole identification criterion $k < 0.5$, suggesting that there is a pole-to-ground fault at the positive pole; At time 1.320 s, fault identification criterion $Q_t < 0.09$C, indicating that the fault is an external one.

The sign of the distributed capacitance value at the positive pole is positive, which is opposite to that of the negative pole, indicating opposite directions of the corresponding capacitance currents, but the analysis method for the fault current and charge transfer is the same as that in Section IV. Therefore, the positive current direction of the negative line can be set as flowing out of the node or generalized node, which can ensure that the same setting value of the identification criterion when applied to both the positive pole and the negative pole.

Set the external negative pole-to-ground fault at f_3 on line l_1 and the results are as shown in Fig.13.

As can be seen from Fig.13, when there is an external negative grounding fault in l_1, initiation criterion $\Delta u > 2kV$, and the protection starts; fault-pole identification criterion $k > 2$, suggesting that there is a pole-to-ground fault at the negative pole; At time 1.320 s, fault identification criterion $Q_t < 0.09$C, indicating that the fault is an external one.

In order to verify the applicability of the protection method to faults with transitional resistance, lots of simulations have been carried out under different conditions in terms of the fault pole, fault position and transitional resistance. The simulation results are shown in Table 3.

The simulation results from Fig.11, Fig.12, Fig.13 and Table 3 show that the protection criterion based on the transferred charges of the differential current can reliably distinguish the internal fault from the external fault, and locate the fault effectively and accurately when a transitional resistance grounding fault occurs.

B. APPLICABILITY TO OVERHEAD LINES

From the parameter comparison in Section II, we can see that the capacitance-to-ground parameters of overhead lines is much smaller than those of cable lines, which is determined by the line structure and material. In order to verify the applicability of the protection algorithm when the overhead

TABLE 3. Simulation results with transitional resistance.

Fault type	Fault pole	Transitional resistance / Ω	Fault pole identification result	Setting value for transferred charge /C	Calculated value of transfer charge /C	Fault location result
Fault in line l_2	Positive pole	100	Positive pole	0.09	0.1588	Internal
		200	Positive pole	0.09	0.1579	Internal
	Negative pole	100	Negative pole	0.09	0.1589	Internal
		200	Negative pole	0.09	0.1579	Internal
Fault in line l_3	Positive pole	100	Positive pole	0.09	-0.0302	External
		200	Positive pole	0.09	-0.0301	External
	Negative pole	100	Negative pole	0.09	-0.0302	External
		200	Negative pole	0.09	-0.0301	External
Fault in line l_1	Positive pole	100	Positive pole	0.09	-0.0302	External
		200	Positive pole	0.09	-0.0301	External
	Negative pole	100	Negative pole	0.09	-0.0302	External
		200	Negative pole	0.09	-0.0301	External

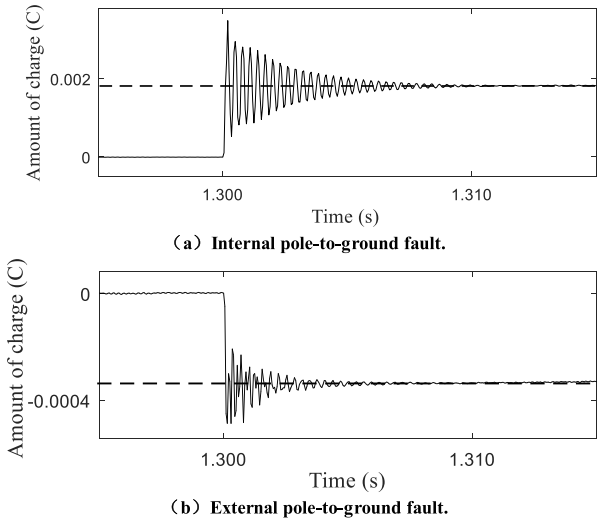

FIGURE 14. Pole-to-ground faults on overhead lines.

lines are adopted in DC distribution networks, the internal and external positive grounding faults are simulated, as shown in Fig.14.

Fig.14 shows that the amount of transferred charges is close to zero when the system is in normal operation, and when a fault occurs, it rises or falls. The amount of the line capacitance transferred charges is smaller than that of the cable line. The amount of transferred charges is about 0.002 C after an internal fault and about −0.0004 C after an external fault. the difference in terms of amount is still obvious.

As long as the measuring elements of protection devices are precise enough, the protection principle proposed in this paper is also applicable to overhead lines

VII. CONCLUSION

By analyzing the transient characteristics of the pole-to-ground fault in cable lines in the DC distribution network, the line capacitance transferred charges calculated according to the line differential current can represent the difference between the internal fault and the external fault. Based on this, the protection criterion for the pole-to-ground fault in DC distribution networks based on capacitance transferred charges is proposed. The conclusions are as follows:

(1) After a pole-to-ground fault, the fault current is mainly composed of the capacitance-to-ground charging and discharging currents of the positive and negative lines and the fault loop current of the system grounding point;

(2) Calculate the amount of the line capacitance transferred charge based on the transient differential current. In the case of an internal fault, the amount of line transferred charges calculated by integrating the differential current is the sum of the capacitance charging charges at the non-fault pole of all lines and the capacitance discharging charges at the fault pole of the external line; In the case of an external fault, the amount of line transferred charges is the negative value of the line capacitance discharging charges of the protected internal line. The difference between the two values is obvious;

(3) The protection principle can distinguish the internal fault from the external fault and will not be affected by the fault transitional resistance;

(4) The protection criterion is easy to set with a definite method, so the usually needed DC line simulation can be saved.

REFERENCES

[1] S. Daniel and S. Ambra, "Low-voltage DC distribution system for commercial power systems with sensitive electronic loads," *IEEE Trans. Power Del.*, vol. 22, no. 3, pp. 1620–1627, Jul. 2007.

[2] N. H. Van Der Blij, L. M. Ramirez-Elizondo, M. T. J. Spaan, and P. Bauer, "Stability and decentralized control of plug-and-play DC distribution grids," *IEEE Access*, vol. 6, pp. 63726–63736, 2018.

[3] T. Dragicevic, J. C. Vasquez, J. M. Guerrero, and D. Skrlec, "Advanced LVDC electrical power architectures and microgrids: A step toward a new generation of power distribution networks," *IEEE Electrific. Mag.*, vol. 2, no. 1, pp. 54–65, Mar. 2014.

[4] T. Kaipia, P. Salonen, J. Lassila, and J. Partanen, "Application of low voltage DC-distribution system—A techno-economical study," in *Proc. 19th Int. Conf. Electr. Distrib.*, May 2007, pp. 1–4.

[5] S. Dhar and P. K. Dash, "Differential current-based fault protection with adaptive threshold for multiple PV-based DC microgrid," *IET Renew. Power Gener.*, vol. 11, no. 6, pp. 778–790, May 2017.

[6] Q. Huai, k. Liu, L. Qin, X. Liao, S. Zhu, Y. Li, and H. Ding, "Backup-protection scheme for multi-terminal HVDC system based on wavelet-packet-energy entropy," *IEEE Access*, vol. 7, pp. 49790–49803, 2019.

[7] D. Jiang and H. Zheng, "Research status and developing propect of DC Distribution network," *Automat. Electron. Power Sys.*, vol. 36, no. 8, pp. 98–104, Apr. 2012.

[8] H. Kakigano, Y. Miura, and T. Ise, "Low-voltage bipolar-type dc microgrid for super high quality distribution," *IEEE Trans. Power Electron.*, vol. 25, no. 12, pp. 3066–3075, Dec. 2010.

[9] S. Arash and M. Kazem, "Studying grounding arrangements of the LVDC system through simulation," *Simulation*, vol. 94, no. 5, pp. 441–449, May 2018.

[10] J. Yang, J. E. Fletcher, and J. O'Reilly, "Short-circuit and ground fault analyses and location in VSC-based DC network cables," *IEEE Trans. Ind. Electron.*, vol. 59, no. 10, pp. 3827–3837, Oct. 2012.

[11] Z. Dai, C. Zhang, X. Chen, and Y. Li, "Fault analysis of multi-terminal flexible DC distribution system with RES," in *Proc. IEEE PES Asia–Pacific Power Energy Eng. Conf. (APPEEC)*, Oct. 2018, pp. 1–6.

[12] M. Lu, "Fundamental-frequency reactive circulating current injection for capacitor voltage balancing in hybrid-MMC HVDC systems during riding through PTG faults," *IEEE Trans. Power Del.*, vol. 33, no. 3, pp. 1348–1357, Jun. 2016.

[13] C. Li, A. M. Gole, and C. Zhao, "A fast DC fault detection method using DC reactor voltages in HVDC grids," *IEEE Trans. Power Del.*, vol. 33, no. 5, pp. 2254–2264, Oct. 2018.

[14] Y. Xu, J. Liu, and Y. Fu, "Fault-line selection and fault-type recognition in DC systems based on graph theory," *Protection Control Modern Power Syst.*, vol. 3, no. 27, pp. 267–276, Dec. 2018.

[15] Y.-C. Liu, and C.-Y. Lin, "Insulation fault detection circuit for ungrounded DC power supply systems," in *Proc. SENSORS*, Oct. 2012, pp. 1–4.

[16] X. Jia, C. Zhao, and B. Li, "Affection of distributed capacitance on and a new method of detecting on detecting DC system earth fault," in *Proc. Int. Conf. Power Syst. Technol.*, Beijing, China, Aug. 1998, pp. 1168–1172.

[17] T. Bi, S. Wang, and K. Jia, "Single pole-to-ground fault location method for MMC-HVDC system using active pulse," *IET Gener., Transmiss. Distrib.*, vol. 12, no. 2, pp. 272–278, Jan. 2018.

[18] Z. Dai, H. Ge, Y. Sq, Z. Wang, and X Chen, "Fault analysis of flxible DC distribution system," *Trans. China Electrotechnical Soc.*, vol. 33, no. 8, pp. 1863–1874, Apr. 2018.

[19] T. Bi, S. Wang, and K. Jia, "Short-term energy based approach for monopolar grounding line identification in MMC–MTDC system," *Power Sys. Technol.*, vol. 40, no. 3, pp. 589–695, Mar. 2016.

[20] G. Song, J. Luo, S. Gao, X. Wang, and K. Tassawar, "Detection method for single-pole-grounded faulty feeder based on parameter identification in MVDC distribution grids," *Int. J. Elect. Power Energy Syst.*, vol. 97, pp. 85–92, Apr. 2018.

[21] S. Debnath, J. Qin, B. Bahrani, M. Saeedifard, and P. Barbosa, "Operation, control, and applications of the modular multilevel converter: A review," *IEEE Trans. Power Electron.*, vol. 30, no. 1, pp. 37–53, Jan. 2014.
[22] G. Sun, B. Shi, and Y. Zhao, "Research on the fault location method and protection configuration strategy of MMC based DC distribution grid," *Power Syst. Protection Control*, vol. 43, no. 22, pp. 127–133, Nov. 2015.
[23] H. Wang, G. Tang, Z. He, and J. Yang, "Efficient grounding for modular multilevel HVDC converters (MMC) on the AC side," *IEEE Trans. Power Del.*, vol. 29, no. 3, pp. 1262–1272, Jun. 2014.
[24] B. T. Li, Y. C. Liu, B. Li, Y. K. Zhang, J. F. Jia, and F. J. Jing, "Development process and analytical method of the pole-to-pole DC fault in the MMC-MVDC system," *IET Power Electron.*, vol. 10, no. 15, pp. 2085–2091, Dec. 2017.
[25] S. S. Wang, X. X. Zhou, G. F. Tang, Z. He, L. Teng, and H. L. Bao, "Analysis of submodule overcurrent caused by DC pole-to-pole fault in modular multilevel converter HVDC system," *Proc. Chin. Soc. Elect. Eng.*, vol. 31, no. 1, pp. 1–8, Jan. 2011.
[26] H. E. Jiawei, L. I. Bin, L. I. Ye, Q. Hong, W. Changqi, and D. Dongkang, "A fast directional pilot protection scheme for the MMC-based MTDC grid," *Proc. Chin. Soc. Elect. Eng.*, vol. 37, no. 23, pp. 6878–6887, Dec. 2017.

BOTONG LI was born in Baoding, China. He received the B.S., M.S., and Ph.D. degrees in electrical engineering from Tianjin University, Tianjin, China, in 2004, 2007, and 2010 respectively.

From 2010 to 2014, he was a Lecturer with the School of Electrical Engineering and Automation, Tianjin University, where he has been an Associate Professor with the School of Electrical and Information Engineering, since 2014. From 2013 to 2014, he was a Research and Development Engineer with the Innovation and Technology Department, Alstom Gird U.K. Ltd. He holds ten patents. He has authored or coauthored more than 40 papers. He was responsible for more than ten national or provincial projects. His main research fields include the protection and control of DC and AC power systems.

XIANG REN received the B.S. degree in electrical engineering from China Agricultural University, Beijing, China, in 2017.

He is currently pursuing the M.S. degree in electrical engineering with Tianjin University, Tianjin, China. His current research interests include the protection and modeling of DC distribution systems.

BIN LI received the B.S., M.S., and Ph.D. degrees in electrical engineering from Tianjin University, Tianjin, China, in 1992, 2002, and 2005, respectively, where he is currently a Professor with the School of Electrical Engineering and Automation.

His main research fields include the protection and control of power systems and microgrids.